

Efficient Self-Supervised Adaptation for Medical Image Analysis

Moein Sorkhei^{1,2} * Emir Konuk^{1,2} Jingyu Guo^{1,2} Christos Matsoukas^{1,2}
Kevin Smith^{1,2}

¹ KTH Royal Institute of Technology, Stockholm, Sweden

² Science for Life Laboratory, Stockholm, Sweden

Abstract. Self-supervised adaptation (SSA) improves foundation model transfer to medical domains but is computationally prohibitive. Although parameter efficient fine-tuning methods such as LoRA have been explored for supervised adaptation, their effectiveness for SSA remains unknown. In this work, we introduce efficient self-supervised adaptation (ESSA), a framework that applies parameter-efficient fine-tuning techniques to SSA with the aim of reducing computational cost and improving adaptation performance. Among the methods tested, Attention Projection Layer Adaptation (APLA) sets a new state-of-the-art, consistently surpassing full-parameter SSA and supervised fine-tuning across diverse medical tasks, while reducing GPU memory by up to 40.1% and increasing training throughput by 25.2%, all while maintaining inference efficiency.

Keywords: Efficient adaptation · Vision transformer · Self-supervised learning.

1 Introduction

Foundation models pretrained on diverse, large-scale natural scene datasets have shown remarkable effectiveness in medical imaging [2,10]. However, their direct transfer is hindered by domain shifts, as natural and medical images differ significantly in structure and content [1,22,19]. Transfer learning, or supervised adaptation (SA), helps bridge this gap by fine-tuning the model weights to the new domain. Further gains can be achieved by first applying self-supervised adaptation (SSA), where the model is pretrained on unlabeled images from the target domain before fine-tuning using supervision [1,14,24,18,27]. A drawback of SSA is its high computational demand, requiring significant memory and long training times [1], which makes it impractical for large foundation models.

Parameter efficient fine-tuning (PEFT) methods such as LoRA [9] and VPT [11] have been developed to reduce the costs of SA, but it remains to be seen whether these methods can effectively optimize the objectives of SSA without degrading the representation quality. In this paper, we introduce this setting of

* Corresponding author: Moein Sorkhei <sorkhei@kth.se>

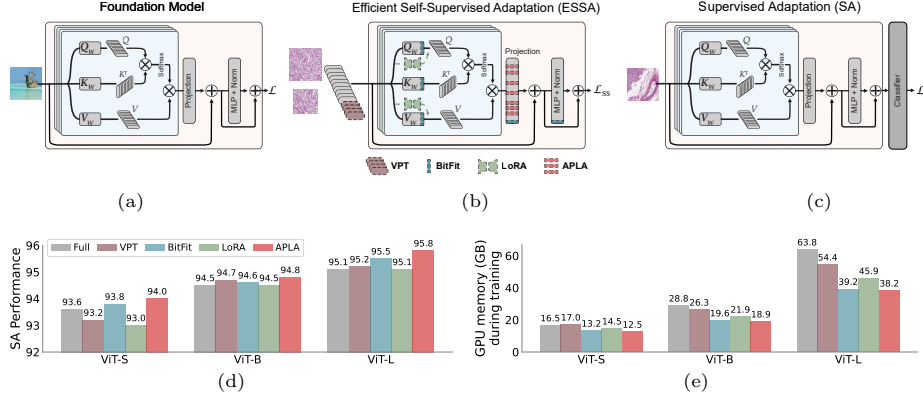


Fig. 1. (Top) The workflow for ESSA. (a) Starting with a foundation model, (b) we investigate different PEFT methods for efficient self-supervised adaptation (ESSA) to adapt the model to the target domain, (c) followed by full-parameter supervised fine-tuning to the target task (SA). (Bottom) (d) performance and (e) GPU memory consumption of PEFT methods during ESSA compared to full-parameter SSA.

efficient self-supervised adaptation (ESSA), where PEFT techniques are applied to SSA with the aims of reducing computational cost and enhancing downstream performance. We evaluate several state-of-the-art methods for ESSA over a variety of medical imaging tasks. We find that for sufficiently large foundation models, ESSA outperforms full-parameter SSA, challenging assumptions behind the current practice of full-network fine-tuning.

Among the methods we tested, APLA [23] is the only PEFT approach that consistently outperforms full-parameter SSA across all settings. APLA is a PEFT strategy that fine-tunes a subset of parameters of the attention projection layers, targeting only the most critical components for adaptation. Our results show that APLA surpasses full-parameter SSA across all classification and segmentation tasks, and establishes a new state-of-the-art. At the same time, APLA reduces GPU memory consumption by up to 40.1% and increases training throughput by 25.2%, without affecting inference costs.

Beyond SSA, we find that applying APLA during both supervised adaptation (SA) and test-time training (TTT) [25] improves model performance and computational efficiency better than other PEFT methods.

Our contributions are as follows: (1) We systematically evaluate PEFT methods applied both for SSA and SA, demonstrating that they improve performance over full-parameter SSA as well as SA for sufficiently large foundation models. (2) We identify APLA [23] as the state-of-the-art ESSA method, consistently surpassing full-parameter SSA across multiple medical imaging tasks while reducing GPU memory usage and increasing training throughput. (3) We show that ESSA methods outperform full-parameter tuning in test-time training (TTT), making them particularly effective in low-label settings.

We share the code to reproduce the results at github.com/MoeinSorkhei/APLA.

2 Related Work

Supervised adaptation (SA), or transfer learning from models pretrained on natural image datasets, is widely used in medical imaging due to the scarcity of labeled data [2,10]. However, this approach faces two major challenges: (1) a domain gap between natural and medical images, which limits transfer learning performance [1,19,22], and (2) the growing computational burden as foundation models [2] become more widely adopted and continue to scale in size [20,6].

SSA offers improved performance by self-supervised training on unlabeled images from the target domain before supervised adaptation [1,14,24,18,27], with the added benefit of avoiding the problem of label scarcity. SSA methods in the past have relied on task-specific pretext tasks [5], adversarial learning [28], or feature alignment [30] but more recently, task-agnostic self-supervised approaches, such as contrastive [1] and discriminative [17] learning, have demonstrated strong performance and broad applicability for SSA with foundation models. Despite their success, these methods significantly increase computational demands when adapting large-scale models [1].

To mitigate the computational costs of full fine-tuning, PEFT methods have been widely explored in SA. Techniques such as LoRA [9], VPT [11], BitFit [29], and APLA [23] have successfully lowered resource requirements by limiting the number of trainable parameters. While these methods effectively reduce training costs for supervised fine-tuning, they are not guaranteed to be effective for SSA, as the objective is to learn reusable, domain-general representations rather than task-specific ones, which means that adapting fewer parameters could be risky, *i.e.*, it might harm general feature learning. To the best of our knowledge, the use of PEFT strategies for SSA have not been systematically investigated until now.

3 Methods

We propose efficient self-supervised adaptation (ESSA), a parameter-efficient adaptation strategy for foundation models in medical imaging. ESSA applies PEFTs in the context of a two-stage foundation model adaptation framework. This starts from a pretrained foundation model depicted in Figure 1a:

1. **Self-Supervised Adaptation (SSA)**: The foundation model is first adapted to the target domain using task-agnostic self-supervised learning on unlabeled images (Fig. 1b).
2. **Supervised Adaptation (SA)** The domain-adapted model is then fine-tuned with an added predictor on labeled data for downstream tasks (Fig. 1c).

We extend the benefits of PEFTs beyond this two-stage framework by exploring their use in test-time training (TTT) [25] as an optional step that allows dynamic adaptation to unlabeled out-of-domain samples during inference.

Two-stage SSA and SA adaptation framework. *We begin by describing the two-stage adaptation framework shown in Figure 1 without incorporating*

parameter-efficient fine-tuning (PEFT). The first stage (Fig. 1b) aligns the foundation model’s representations with the medical domain using self-supervised learning.

This enables the model to learn rich representations from the target domain, but it is task-agnostic, limiting its ability to support diagnostic tasks.

This necessitates a second stage (Fig. 1b), supervised adaptation (SA), where a classifier or task-specific head is added to the domain-adapted feature extractor from stage one. The model is then fine-tuned using supervised learning on image-label pairs to optimize task performance.

Parameter-efficient fine-tuning (PEFT). Full fine-tuning of large foundation models is computationally expensive. To mitigate this cost, PEFT methods update only a small subset of parameters while keeping most of the model frozen. These approaches fall into two broad categories: additive methods [9,11], which introduce additional trainable components without modifying the backbone, and parameter-selective methods [29,23] which fine-tune a limited subset of existing model weights. *While PEFT has been successfully applied for standard transfer learning, its effectiveness for SSA remains unexplored.*

Efficient self-supervised adaptation (ESSA). We apply PEFT techniques to SSA (and, optionally SA) optimizing only a small set of parameters, γ , instead of the full foundation model parameters. The general form of the efficient SSA step (ESSA) is given by

$$\min_{\gamma} \mathcal{L}_{SS} \left(F_{\phi^*, \gamma}(x) \right) \quad (1)$$

which yields a model \hat{F} adapted to the target domain. This is followed by an SA step, which can optionally also be made efficient with PEFTs by

$$\min_{\theta, \gamma} \mathcal{L}_S \left(y, h_{\theta}(\hat{F}_{\phi^*, \gamma}(x)) \right) \quad (2)$$

where h denotes a prediction head with parameters θ . We use \mathcal{L}_{SS} to indicate a self-supervised objective calculated on images $x \sim \mathcal{D}$ from the target dataset, and \mathcal{L}_S is a supervised loss function calculated on image-label pairs $(x, y) \sim \mathcal{D}$ from the same dataset¹.

For some efficient adaptation methods like LORA [9] and VPT [11], all parameters of the foundation model F_{ϕ} are frozen, $\phi^* = \phi$, and the tunable parameters γ represent the additional parameters injected to the model. For LORA [9], these are low-rank matrix approximations to the changes in model parameters during adaptation, whereas for VPT [11] they are a learnable prompt vector prepended to the foundation model. For other efficient methods like BITFIT [29] and APLA [23], tunable γ parameters represent a subset of the foundation model parameters, $\phi = \phi^* \cup \gamma$, while the rest, ϕ^* , are kept frozen. For BITFIT

¹ Note that frozen ϕ^* and tunable parameters γ of the foundation model F and domain adapted model \hat{F} can be different, *e.g.*, a different adapter block or a different subset of existing parameters may be tuned during the SSA and SA stages.

[29], the tuneable subset γ are the bias terms while APLA [23] selectively fine-tunes a random subset of the parameters in the layer immediately following the attention mechanism, which its authors identified as critical for adaptation.

Test-time training (TTT). Test-time training is a self-supervised domain adaptation method [25,8] that updates the feature extractor during inference using self-supervised learning, while keeping the classifier fixed. Instead of full-network adaptation, we apply PEFT methods to optimize a small subset of parameters of the feature extractor. This enables efficient on-the-fly adaptation to domain shifts without explicit supervision, making it particularly useful in deployment scenarios common in medical image analysis where distributions shift and labeled samples are unavailable.

4 Experimental setup

Datasets. We experiment with 5 medical image analysis datasets. For classification tasks we use APTOS2019 [12], DDSM [15], and Colorectal [13]. Additionally, we evaluate efficient adaptation methods for TTT [25] by assessing models trained on APTOS2019 and adapted at test time to IDRiD [21], which presents a domain shift in diabetic retinopathy classification. For semantic segmentation, we use ISIC2018 [4,26]. We use the provided standard train/val/test splits and performance metrics when available, otherwise following [23,19]. In all cases, the same data is available for ESSA, SSA, and SA stages.

Implementation details. For self-supervision we use DINOv2 [20] using a ViT [7] backbone. For semantic segmentation we use the SETR-PUP framework [31] with a ViT-L encoder and convolutional decoder. The PEFT methods we consider are LORA [9] which injects low-rank trainable matrices into self-attention layers, VPT [11] which modifies input token embeddings using learnable prompts, BITFIT [29] which fine-tunes only bias terms, and APLA [23] which selectively fine-tunes a small fraction of projection layer weights in self-attention blocks. For ESSA, models are trained for 300 epochs using AdamW [16], with hyperparameters as recommended by [20]. For SA, models are trained for 100 epochs, utilizing a cosine decay schedule with a 10-epoch warm-up. Hyperparameters are selected via grid search on the validation set. ESSA runs on 4 A100 GPUs in a multi-GPU training setup with a total batch size of 256, while SA runs on a single A100 GPU with a batch size of 64.

Evaluation protocols. To evaluate ESSA we follow two widely used evaluation protocols [3,20]: 1) We use a weighted nearest neighbor classifier (k -NN) with the adapted backbone as the feature extractor to evaluate representation quality. 2) A classification head is appended to the adapted backbone, and the entire network undergoes SA. This evaluation framework remains consistent across full-network training and all PEFT methods. For test-time training, the classification head trained with SA is frozen and used for prediction on test data after applying ESSA to adapt the feature extractor to the test data.

Table 1. Comparison of various PEFT methods for ESSA.

Method	Foundation model	APTOS		DDSM		Colorectal		Average	
		<i>k</i> -NN	SA	<i>k</i> -NN	SA	<i>k</i> -NN	SA	<i>k</i> -NN	SA
Standard transfer learning	ViT-S + DINO V2	77.2	88.9	85.9	92.8	87.0	96.0	83.4	92.6
FULL parameter SSA	ViT-S + DINO V2	80.6	89.9	88.3	94.1	92.6	96.8	87.2	93.6
ESSA with VPT [11]	ViT-S + DINO V2	69.5	89.6	88.6	93.7	89.2	96.4	82.4	93.2
ESSA with BrrFit [29]	ViT-S + DINO V2	81.1	90.2	89.3	94.3	92.0	96.8	87.5	93.8
ESSA with LoRA [9]	ViT-S + DINO V2	81.7	89.4	87.9	93.5	92.8	96.2	87.5	93.0
ESSA with APLA [23]	ViT-S + DINO V2	84.0	90.2	91.0	94.9	93.6	96.8	89.5	94.0
Standard transfer learning	ViT-B + DINO V2	79.0	90.2	86.6	95.1	88.8	97.8	84.8	94.4
FULL parameter SSA	ViT-B + DINO V2	81.3	90.4	88.7	95.2	93.4	98.0	87.8	94.5
ESSA with VPT [11]	ViT-B + DINO V2	77.4	90.5	88.7	95.3	92.0	98.2	86.0	94.7
ESSA with BrrFit [29]	ViT-B + DINO V2	82.3	90.5	89.7	95.3	94.0	98.0	88.7	94.6
ESSA with LoRA [9]	ViT-B + DINO V2	82.1	90.5	89.5	95.0	93.4	98.0	88.3	94.5
ESSA with APLA [23]	ViT-B + DINO V2	84.8	90.8	91.9	95.4	94.6	98.2	90.4	94.8
Standard transfer learning	ViT-L + DINO V2	81.2	90.5	88.2	96.3	89.6	98.0	86.3	94.9
FULL parameter SSA	ViT-L + DINO V2	83.7	90.9	89.3	96.5	94.2	98.0	89.1	95.1
ESSA with VPT [11]	ViT-L + DINO V2	78.6	91.4	89.2	96.2	94.6	98.0	87.5	95.2
ESSA with BrrFit [29]	ViT-L + DINO V2	85.2	91.9	90.1	96.7	95.0	97.8	90.1	95.5
ESSA with LoRA [9]	ViT-L + DINO V2	82.2	90.6	89.8	96.6	96.6	98.2	89.5	95.1
ESSA with APLA [23]	ViT-L + DINO V2	86.9	91.9	92.7	97.0	96.2	98.4	91.9	95.8
FULL parameter SSA	ViT-L + IMAGENET-21K	83.1	89.0	88.9	93.7	95.2	97.8	89.1	93.5
ESSA with VPT [11]	ViT-L + IMAGENET-21K	79.8	89.2	89.4	94.4	95.2	97.8	88.1	93.8
ESSA with BrrFit [29]	ViT-L + IMAGENET-21K	80.1	89.6	90.4	94.4	94.4	97.6	88.3	93.9
ESSA with LoRA [9]	ViT-L + IMAGENET-21K	79.6	88.8	88.2	93.4	95.2	96.4	87.7	92.9
ESSA with APLA [23]	ViT-L + IMAGENET-21K	83.2	89.8	90.5	94.6	96.6	98.0	90.1	94.1
Standard transfer learning	ViT-L + DINO V2	-	90.5	-	96.3	-	98.0	-	94.9
ESSA with VPT [11]	ViT-L + DINO V2	-	91.1*	-	97.9*	-	98.2*	-	95.7*
ESSA with BrrFit [29]	ViT-L + DINO V2	-	90.5*	-	97.0*	-	97.8*	-	95.1*
ESSA with LoRA [9]	ViT-L + DINO V2	-	91.2*	-	97.4*	-	98.2*	-	95.6*
ESSA with APLA [23]	ViT-L + DINO V2	-	92.0*	-	97.1*	-	98.6*	-	95.9*

* indicates supervised adaptation (SA) is also performed with PEFT.

5 Results

Main results. Our main results in Table 1 demonstrate that efficient adaptation methods offer, on average, an improvement in downstream performance over full-parameter SSA, but the gains are not consistent across PEFT methods. *APLA is the only PEFT method that consistently outperforms both standard transfer learning and full-parameter SSA across all tasks, architectures, and evaluation protocols.* Representation quality, as measured by *k*-NN paints a similar picture, where most ESSA methods (aside from VPT) learn better representations than full-parameter SSA. We observe a trend of diminishing returns from full-parameter SSA as the foundation model grows, while ESSA methods continue to improve adaptation performance. For sufficiently large models, ESSA is universally better than SSA. Notably, while all PEFT approaches benefit from larger foundation models, APLA remains the only method that consistently surpasses full-parameter SSA across all cases. This trend persists when using a ViT-L pretrained on IMAGENET-21K. When we apply the PEFT methods to both the SSA and SA steps, we see additional gains in downstream performance for all methods aside from BrrFit, with APLA again dominating.

ESSA for semantic segmentation. Semantic segmentation results on ISIC2018 are given in Figure 3, where ESSA is performed followed by full-parameter SA. Both APLA and VPT outperform full-parameter SSA, while LoRA is on-par and BrrFit underperforms full SSA.

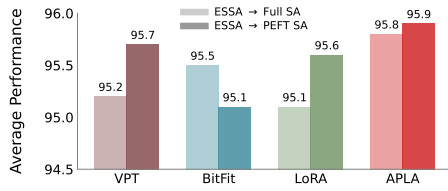


Fig. 2. ESSA followed by efficient SA.

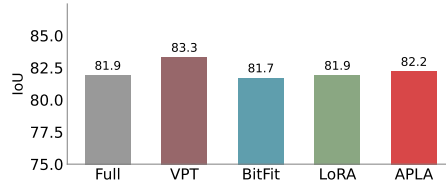


Fig. 3. ESSA for semantic segmentation.

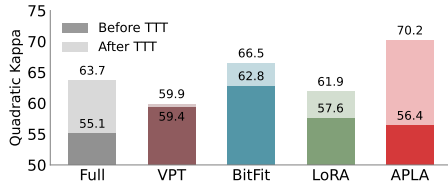


Fig. 4. TTT on OOD data using PEFT.

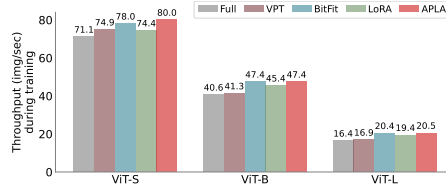


Fig. 5. SSA/ESSA training throughput.

PEFT for test-time training (TTT). In Figure 4 we apply a PEFT method to our entire SSA/SA pipeline on a source domain, then adapt the feature extractor to a new domain at test time [25] using the same PEFT method. Results show the difference between the source-adapted model and the model adapted to the test data using TTT. Among PEFT methods, only APLA [23] brings a performance boost larger than full-parameter tuning.

Computational efficiency. We report GPU memory usage in Figure 1e and training throughput in Figure 5. All PEFT methods improve efficiency, with APLA offering the largest gains – 40.1% savings in GPU memory consumption and 25.2% training speed-up, without affecting inference costs.

6 Discussion

ESSA challenges the assumption that full-parameter SSA is necessary. PEFT methods were originally designed for standard transfer learning (SA), leading to the natural question of whether they are as effective for SSA. One key concern is that optimizing only a small subset of parameters may not be enough during SSA for adapting the rich foundational representations to medical tasks. Our results show that SSA provides diminishing returns for large foundation models, with only marginal improvements over standard supervised transfer learning (SA). This suggests that the primary limitation of SSA for large models is not just the computational cost, but also limited adaptation gains. However, applying PEFTs in ESSA fundamentally shifts this paradigm: once a foundation model is sufficiently large, PEFT methods outperform full-parameter SSA, making ESSA the better strategy. Instead of a costly adaptation step with marginal benefits, ESSA makes SSA both feasible and effective.

APLA is the best ESSA method across all scenarios. While all PEFT methods improve efficiency, we found that APLA is the only approach that consistently brings performance benefits, outperforming full-parameter SSA across all tasks and architectures. By the simple virtue of limiting the number of tunable parameters, APLA is incentivized to better preserve the rich representations of the pretrained foundation models. While other PEFT methods may also be benefiting from this same implicit regularization effect, APLA is unique in that it forces the model to recompose existing features within the critical attention projection layers [23]. This implicit regularization may be particularly beneficial in medical imaging, where data is often scarce, and models risk memorizing low-variance distributions dominated by background pixels.

PEFT enhances domain adaptation at all stages. Beyond SSA, our results demonstrate that PEFT provides the greatest gains when applied to SA and TTT as well as SSA. This result was not trivial at the outset—yet our findings suggest that PEFT is not just an efficiency trade-off, but an actively better approach than full-parameter tuning for domain adaptation. By enforcing structured adaptation, PEFT methods facilitate better feature reuse between SSA and SA, while also improving on-the-fly adaptation in test-time training (TTT). From a practical perspective, this means that PEFT enables performant and computationally efficient medical AI, allowing large foundation models to adapt dynamically, even in resource-constrained deployment settings where labeled data is unavailable.

Implications for Medical AI. The success of ESSA highlights a major shift in how adaptation should be approached for large-scale medical AI. Our results suggest that targeted, efficient adaptation can match or exceed traditional transfer learning and even the more powerful SSA approaches at a fraction of the cost.

Limitations and future work. While our findings establish ESSA as an effective paradigm, there are still open questions. Our study primarily focused on DINOv2 as the self-supervised learning (SSL) objective, as initial experiments showed it to be superior to other SSL methods. However, we did not systematically investigate whether other contrastive or masked image modeling approaches might yield different adaptation behaviors with PEFT. Future work should explore whether certain SSL paradigms are better suited for ESSA and whether additional architectural modifications can further improve adaptation efficiency.

7 Conclusion

In this work we investigate the effectiveness of ESSA for medical image analysis. We show that applying PEFT methods improve the quality of adapted representations and boost downstream performance while reducing computational costs. We identify APLA [23] as the only PEFT method consistently improving SSA performance, with further improvements when applied during supervised transfer learning and test-time training [25]. By demonstrating the effectiveness and efficiency of PEFT methods for self-supervised adaptation,

we aim to make foundation models more accessible to the wider medical image analysis community.

Acknowledgments. This work was supported by the Wallenberg AI, Autonomous Systems and Software Program (WASP). We acknowledge the Berzelius computational resources provided by the Knut and Alice Wallenberg Foundation at the National Supercomputer Centre and the the computational resources provided by the National Academic Infrastructure for Supercomputing in Sweden (NAISS), partially funded by the Swedish Research Council through grant agreement no. 2022-06725.

References

1. Azizi, S., Mustafa, B., Ryan, F., Beaver, Z., Freyberg, J., Deaton, J., Loh, A., Karthikesalingam, A., Kornblith, S., Chen, T., et al.: Big self-supervised models advance medical image classification. In: Proceedings of the IEEE/CVF international conference on computer vision. pp. 3478–3488 (2021)
2. Bommasani, R., Hudson, D.A., Adeli, E., Altman, R., Arora, S., von Arx, S., Bernstein, M.S., Bohg, J., Bosselut, A., Brunskill, E., et al.: On the opportunities and risks of foundation models. arXiv preprint arXiv:2108.07258 (2021)
3. Caron, M., Touvron, H., Misra, I., Jégou, H., Mairal, J., Bojanowski, P., Joulin, A.: Emerging properties in self-supervised vision transformers. In: Proceedings of the IEEE/CVF international conference on computer vision. pp. 9650–9660 (2021)
4. Codella, N., Rotemberg, V., Tschandl, P., Celebi, M.E., Dusza, S., Gutman, D., Helba, B., Kalloo, A., Liopyris, K., Marchetti, M., et al.: Skin lesion analysis toward melanoma detection 2018: A challenge hosted by the international skin imaging collaboration (isic). arXiv preprint arXiv:1902.03368 (2019)
5. Cui, B., Islam, M., Bai, L., Wang, A., Ren, H.: Endodac: Efficient adapting foundation model for self-supervised depth estimation from any endoscopic camera. In: International Conference on Medical Image Computing and Computer-Assisted Intervention. pp. 208–218. Springer (2024)
6. Dehghani, M., Djolonga, J., Mustafa, B., Padlewski, P., Heek, J., Gilmer, J., Steiner, A.P., Caron, M., Geirhos, R., Alabdulmohsin, I., et al.: Scaling vision transformers to 22 billion parameters. In: International Conference on Machine Learning. pp. 7480–7512. PMLR (2023)
7. Dosovitskiy, A.: An image is worth 16x16 words: Transformers for image recognition at scale. arXiv preprint arXiv:2010.11929 (2020)
8. Gandelsman, Y., Sun, Y., Chen, X., Efros, A.: Test-time training with masked autoencoders. Advances in Neural Information Processing Systems **35**, 29374–29385 (2022)
9. Hu, E.J., Shen, Y., Wallis, P., Allen-Zhu, Z., Li, Y., Wang, S., Wang, L., Chen, W.: Lora: Low-rank adaptation of large language models. arXiv preprint arXiv:2106.09685 (2021)
10. Huix, J.P., Ganeshan, A.R., Haslum, J.F., Söderberg, M., Matsoukas, C., Smith, K.: Are natural domain foundation models useful for medical image classification? In: Proceedings of the IEEE/CVF winter conference on applications of computer vision. pp. 7634–7643 (2024)

11. Jia, M., Tang, L., Chen, B.C., Cardie, C., Belongie, S., Hariharan, B., Lim, S.N.: Visual prompt tuning. In: European Conference on Computer Vision. pp. 709–727. Springer (2022)
12. Karthik, Maggie, S.D.: Aptos 2019 blindness detection (2019), <https://kaggle.com/competitions/aptos2019-blindness-detection>
13. Kather, J.N., Weis, C.A., Bianconi, F., Melchers, S.M., Schad, L.R., Gaiser, T., Marx, A., Zöllner, F.G.: Multi-class texture analysis in colorectal cancer histology. *Scientific reports* **6**(1), 1–11 (2016)
14. Kumari, S., Singh, P.: Deep learning for unsupervised domain adaptation in medical imaging: Recent advancements and future perspectives. *Computers in Biology and Medicine* **170**, 107912 (2024)
15. Lee, R.S., Gimenez, F., Hoogi, A., Miyake, K.K., Gorovoy, M., Rubin, D.L.: A curated mammography data set for use in computer-aided detection and diagnosis research. *Scientific data* **4**(1), 1–9 (2017)
16. Loshchilov, I., Hutter, F.: Decoupled weight decay regularization. *arXiv preprint arXiv:1711.05101* (2017)
17. Matsoukas, C., Haslum, J.F., Söderberg, M., Smith, K.: Is it time to replace cnns with transformers for medical images? *arXiv preprint arXiv:2108.09038* (2021)
18. Matsoukas, C., Haslum, J.F., Söderberg, M., Smith, K.: Pretrained vits yield versatile representations for medical images. *arXiv preprint arXiv:2303.07034* (2023)
19. Matsoukas, C., Haslum, J.F., Sorkhei, M., Söderberg, M., Smith, K.: What makes transfer learning work for medical images: Feature reuse & other factors. In: Proceedings of the IEEE/CVF Conference on Computer Vision and Pattern Recognition. pp. 9225–9234 (2022)
20. Oquab, M., Darcet, T., Moutakanni, T., Vo, H., Szafraniec, M., Khalidov, V., Fernandez, P., Haziza, D., Massa, F., El-Nouby, A., et al.: Dinov2: Learning robust visual features without supervision. *arXiv preprint arXiv:2304.07193* (2023)
21. Porwal, P., Pachade, S., Kamble, R., Kokare, M., Deshmukh, G., Sahasrabudhe, V., Meriaudeau, F.: Indian diabetic retinopathy image dataset (IDRiD): A database for diabetic retinopathy screening research. *Data* **3**(3) (2018). <https://doi.org/10.3390/data3030025>, <https://www.mdpi.com/2306-5729/3/3/25>
22. Raghu, M., Zhang, C., Kleinberg, J., Bengio, S.: Transfusion: Understanding transfer learning for medical imaging. *Advances in neural information processing systems* **32** (2019)
23. Sorkhei, M., Konuk, E., Smith, K., Matsoukas, C.: Apla: A simple adaptation method for vision transformers. *arXiv preprint arXiv:2503.11335* (2025)
24. Sowrirajan, H., Yang, J., Ng, A.Y., Rajpurkar, P.: Moco pretraining improves representation and transferability of chest x-ray models. In: Medical Imaging with Deep Learning. pp. 728–744. PMLR (2021)
25. Sun, Y., Wang, X., Liu, Z., Miller, J., Efros, A., Hardt, M.: Test-time training with self-supervision for generalization under distribution shifts. In: International conference on machine learning. pp. 9229–9248. PMLR (2020)
26. Tschandl, P., Rosendahl, C., Kittler, H.: The ham10000 dataset, a large collection of multi-source dermatoscopic images of common pigmented skin lesions. *Scientific data* **5**(1), 1–9 (2018)
27. Xiao, J., Bai, Y., Yuille, A., Zhou, Z.: Delving into masked autoencoders for multi-label thorax disease classification. In: Proceedings of the IEEE/CVF Winter Conference on Applications of Computer Vision. pp. 3588–3600 (2023)
28. Xu, J., Xiao, L., López, A.M.: Self-supervised domain adaptation for computer vision tasks. *IEEE Access* **7**, 156694–156706 (2019)

29. Zaken, E.B., Ravfogel, S., Goldberg, Y.: Bitfit: Simple parameter-efficient fine-tuning for transformer-based masked language-models. arXiv preprint arXiv:2106.10199 (2021)
30. Zhang, Y., Chen, H., Wei, Y., Zhao, P., Cao, J., Fan, X., Lou, X., Liu, H., Hou, J., Han, X., et al.: From whole slide imaging to microscopy: Deep microscopy adaptation network for histopathology cancer image classification. In: International conference on medical image computing and computer-assisted intervention. pp. 360–368. Springer (2019)
31. Zheng, S., Lu, J., Zhao, H., Zhu, X., Luo, Z., Wang, Y., Fu, Y., Feng, J., Xiang, T., Torr, P.H., et al.: Rethinking semantic segmentation from a sequence-to-sequence perspective with transformers. In: Proceedings of the IEEE/CVF conference on computer vision and pattern recognition. pp. 6881–6890 (2021)